Hindawi
Advances in Civil Engineering
Volume 2019, Article ID 5841840, 13 pages
https://doi.org/10.1155/2019/5841840

Research Article

Field Tests and Simplified Calculation Method for Static Drill Rooted Nodular Pile

Zhong-Jin Wang[1,2] **Ri-Hong Zhang**[3] **Xin-Yu Xie**[1,4] **Peng-Fei Fang**[1,2] **Ling-Wei Zheng**[1,4] **Jin-Zhu Li**[1] **and Da-Yong Zhu**[1,2]

[1]*Ningbo Institute of Technology, Zhejiang University, Ningbo 315100, China*
[2]*Ningbo Research Institute, Zhejiang University, Ningbo 315100, China*
[3]*ZCONE High-tech Pile Industry Holdings Co., Ltd., Ningbo, Zhejiang 315000, China*
[4]*Research Center of Coastal and Urban Geotechnical Engineering, Zhejiang University, Hangzhou 310058, China*

Correspondence should be addressed to Zhong-Jin Wang; zhongjin_wang@zju.edu.cn and Ri-Hong Zhang; zhangrihong5@hotmail.com

Received 22 March 2019; Revised 15 May 2019; Accepted 3 June 2019; Published 26 June 2019

Academic Editor: Cumaraswamy Vipulanandan

In order to explore bearing characteristics of a new-type static drill rooted nodular pile foundation (SDRN), which is composed of PHC pile, bamboo joint pile, and cement soils, field tests of three piles were carried out by embedding internal rebar stress gauges to collect test data. The test results show that the SDRN piles were under elastic state and the load-settlement curves changed slowly before reaching the ultimate capacity. As pile head loads increased, the pile shaft frictions developed progressively, and axial forces gradually reduced along pile depths. Taking into account the interaction between the pile, the cement soils, and surrounding soils, a simplified method for calculating settlements and bearing capacity of SDRN piles was proposed. With corresponding parameters, the computing results obtained by the proposed method were compared with the field experimental data, which indicates acceptable agreements; thus, it is concluded that the applicability and predictive capability of the proposed method were verified.

1. Introduction

With advantages of economical benefits and fast piling speed compared with bored piles, prestressed hollow concrete (PHC) piles are widely used in deep soft soil areas within China recently. However, the shaft friction of PHC pile is always small when used in soft soils, resulting in the ultimate bearing state being easily reached and thereafter large settlements happen. The construction process of PHC pile produces severe soil squeezing effect on the surrounding infrastructure and soils [1, 2]. As a new type of precast reinforced concrete piles, the bamboo joint pile is widely used regarding its effective improvements to bearing behaviors of foundations. However, the similar problems of PHC piles mentioned above also occurred in the process of construction for bamboo joint pile. With insignificant squeezing effects in the process of construction, the static drill rooted nodular pile (SDRN) has been adopted widely in the deep soft soil area of Zhejiang province in China. It is concluded that the static drill rooted nodular pile (SDRN) was firstly used in Japan and then introduced in China [3, 4]; the SDRN pile consists of PHC piles, bamboo joint pile, and surrounding cemented soils. The static drill rooted method is new and environment friendly which has insignificant effects on the surrounding foundations and largely decreases the mud emissions [4–6]. The construction process can be summarized as follows:

(1) Drilling hole: set up the drill machine at the design position and drill the pile hole using a special auger, with controllable drilling speed according to the geological conditions. In the drilling process, the drilling hole is repaired and protected by injecting bentonite slurry of high water content.

(2) Expanding pile end: the drilling machine used here is specially manufactured with an expandable wing which enlarges the diameter at the bottom of the hole to pour the enlarged pile base; the whole process is monitored by the autocontrol system.

(3) Grouting cement slurry at pile end and pile shaft side: lifting the drilling machine up and down repeatedly during the grouting process to ensure that the cement paste is injected into the base of the expanding hole and the cemented soil is successfully formed. Grouting cement slurry at pile side: pulling out the drilling machine and grouting cement slurry at pile side along the hole and stirring repeatedly while pulling out the drilling machine.

(4) Planting: putting the pile into the hole filled with cement slurry after the drilling machine is pulled out. The whole process is monitored to ensure that the pile remains upright and reaches the target depth. The construction process of the static drill rooted nodular pile is also shown in Figure 1.

In order to study the bearing characteristics of static drill rooted pile under vertical load, full-scale destructive and nondestructive field tests on three static drill rooted piles were carried out. The tested piles were attached with strain gauges to investigate the load transfer mechanism of static drill rooted piles. The load settlements and the distribution of axial forces were obtained from the field tests, indicating important bearing characteristics of this new-type pile foundations.

To estimate pile settlements and simulate load transfer mechanism between pile shaft and surrounding soils, various methods have been proposed to predict the bearing capacity and settlement of pile foundation under vertical loads during the past few decades. However, the research works on the calculation methods for this new-type pile (SDRN) are believed far behind the engineering practice so far. Many researchers proposed simplified analytical methods, considering the relative displacement between pile shaft and surrounding soils [7–10]. Using load transfer functions to describe pile-soil interaction behavior, the transfer-function method was proposed to describe load transfer mechanism by Seed and Reese [11] and later was extended by many other investigators [10, 12, 13]. Even though the abovementioned methods have many superiorities in analysis of settlement and load transfer mechanism for single pile, they are not suitable for this new-type composite pile (SDRN) and are not applicable due to the interaction between PHC pile, bamboo joint pile, surrounding soils, and cement soil. Regarding the complex mechanism of interaction between piles and surrounding soils, the most reliable method to assess single pile response under vertical loads must be field-scale static pile load test. However, high cost and time consumption are problems resulted from the in situ static pile load tests. Meanwhile, simplified methods that allow for rapid estimation of bearing characteristics for a single pile of this new-type pile (SDRN), and the nonlinearity between cement soils and surrounding soils, are rarely available in engineering practice. The objective of this paper is to obtain a better understanding of the behavior of the static drill rooted nodular pile (SDRN) based on the analysis of field tests, and proposes a simplified calculation method to predict the bearing capacity and settlements for this new type pile, considering the interaction of pile, cement soils, and surrounding soils. Through comparisons between calculated and field tests results, analyzed results indicate that the proposed method is sufficiently accurate to predict the behavior of this new-type pile foundation.

2. Field Conditions and Test Pile Description

Three static drill rooted nodular piles were tested in field, and rebar stress gauges used for measurement of reinforcement stress in reinforcing cage were embedded in the piles during the manufacturing process in the workshop, and good protection was obtained during construction, as shown in Figure 2. The rebar stress gauges were arranged at 1.5 m, 18 m, 28 m, 39 m, 46.5 m, and 53.5 m below the head of test piles, respectively, and every embedded section position had a set of four gauges, as shown in Figure 3(a).

For optimal design, a composite pile combining a PHC pile in the upper section with a matched bamboo joint of the pile in the lower section was used in test piles, as shown in Figure 3(b). The size of nodular piles used in the field tests was: 650–500 (100) mm at the lower part of the static drill rooted nodular piles for 15 m and 600 (110) mm at the upper part of the pile for 40 m. The detailed meaning of the 650-500 (100) mm type is that the external diameter of bamboo joint in the pile is 650 mm, the external diameter of the other parts is 500 mm, and the wall thickness of pile is 100mm. The 600 (110) mm means that the outside diameter of pile is 600 mm and the wall thickness of pipe pile is 110 mm. The detailed meaning of the above dimensions is also shown in Figure 3(b).

The field tests were conducted in Shanghai, China, and three static drill rooted nodular piles were tested on the same site. The field soil geotechnical properties and parameters are shown in Table 1.

The field tests were conducted according to the slow maintenance load method, described in the Chinese Technical Code for Testing of Building Foundation Piles [14]. The load was applied by the reaction of jacks at the pile top and was increased step by step. The magnitude of load at each step was selected as 1/8~1/12 of the maximum design load for the test, and the magnitude of the first load step was double that of the subsequent load steps. At each load step, the settlement at the pile head was recorded after the load had been applied and maintained for 5, 15, 30, 45, and 60 min. Thereafter, the settlement was recorded every 30 min. Each load increment was maintained after loading until two consecutive displacements within each hour were less than 0.1 mm. The unloading test was performed by reducing the load in decrements that were twice the loading increments. These requirements were based on the typical criteria recommended by the Chinese Technical Code for Testing of Building Foundation Piles [14]. Tested pile counterforces were provided by surcharge-load reaction

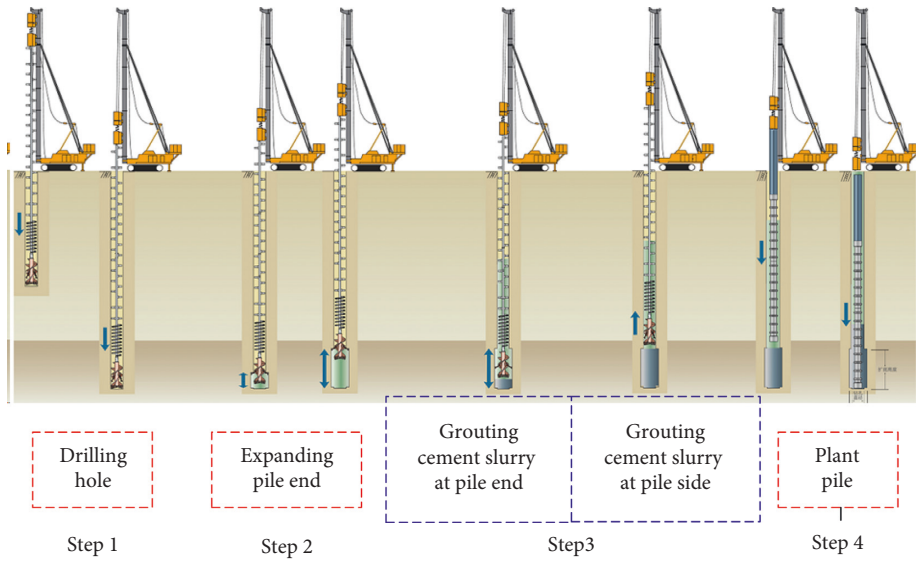

Figure 1: Construction process of static drill rooted pile.

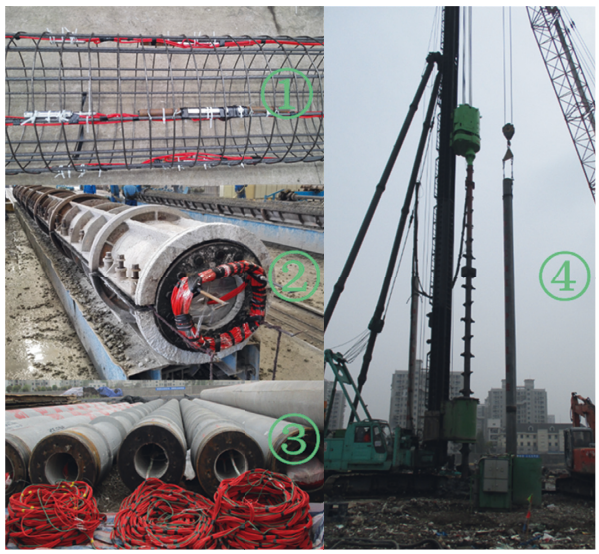

Figure 2: Manufacturing process.

frame and hydraulic jack measuring system. The static load test system for pile foundation was adopted to measure and collect data from the rebar stress gauges.

The borehole diameter is 750 mm for the three test piles. The expanding diameter at the pile bottom is 1200 mm, and the expanding length is 2750 mm for the three tested piles. In process of drilling construction, the drilling rate of the bit is automatically controlled by the automatic monitoring system according to the collected data of automatic devices. The detailed parameters for the tested piles are shown in Table 2.

3. Results of Static Load Tests

3.1. Load-Displacement Responses of Piles. The ultimate bearing capacity of a single pile can be defined as the load when displacement at the pile head increased rapidly under sustained load. Punching failure typically involves pile head settlements that far exceed the acceptable range for design code. If the plunging point is not clear, the ultimate load can be obtained by the analysis of the load-displacement curve. The load-displacement curve is a useful tool to establish the ultimate bearing capacity of a single pile under compression load. The vertical compressive static load testes were carried out 45 days after the installation of the tested piles constructions, adopting slow maintenance surcharge-load method according to the Chinese Technical Code for Testing of Building Foundation Piles [14]. The load-settlement curves for the three tested piles are shown in Figure 4.

From Figure 4, it can be seen that test pile of S-1 is loaded to 8800 kN, and the cumulative settlement is 36.65 mm and stable. The applied load is continued increasing to 9600 kN, and the load-settlement curves of test pile S-1 show a sharp drop. The ultimate bearing capacity of the test pile S-1 is determined as 8800 kN. The test pile S-2 is loaded to 8000 kN, and the cumulative settlement is 24.01 mm and stable, so the ultimate bearing capacity of the test pile S-2 is not less than 8000 kN. The test pile S-3 is loaded to 8800 kN, and the cumulative settlement is 35.70 mm and stable. The applied load at S-3 pile head is then continued increasing to 9600 kN, and the load-settlement curves of the test pile S-3 also show a sharp drop as test pile S-1, and the ultimate bearing capacity of the test pile S-3 is also determined to be 8800 kN.

After the static load tests, the test piles start to unload, and the unloading-displacement curves are also shown in Figure 4. The residual settlements for the tested piles S-1, S-2, and S-3 are 26.96 mm, 2.50 mm, and 26.16 mm, respectively, and the rebounded rates for the above three tested piles are 63.3%, 89.6%, and 68.1%, respectively.

3.2. Axial Forces and Side Frictions of Test Piles. As mentioned above, the tested piles are equipped with rebar stress gauges, and the average axial forces of the tested piles can

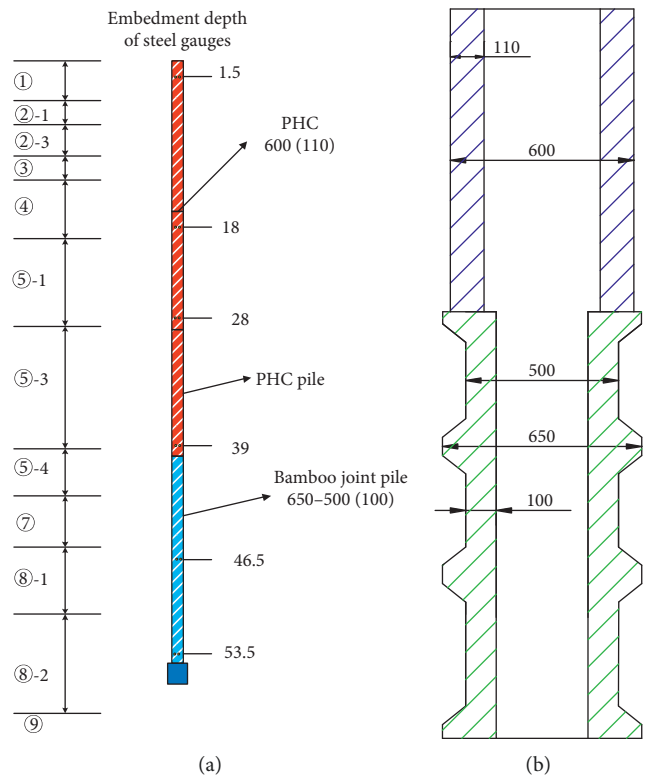

Figure 3: Embedding gauges and geometry size of test piles. (a) Embedding gauges of test piles. (b) Composition form of static drill rooted nodular pile (unit: mm).

Table 1: Soil profile and parameters for the tested piles.

Number of layers	Name of soil layer	Elevation at bottom of layers (m)	Thickness of soil layer (m)	Specific penetration resistance (m)	Value of ultimate friction resistance of pile side (kPa)	Ultimate friction resistance of pile end (kPa)
①-1	Miscellaneous fill	1.09	1.09		15	
②-1	Silty clay	−0.31	1.4	0.65	40	
②-3	Sandy silty soil	−3.61	3.3	2.75	15	
③	Muddy silty clay	−7.51	3.9	0.46	25	
④	Muddy clay	−17.04	9.53	0.61	40	
⑤-1	Silty clay	−25.41	8.37	1.04	55	
⑤-3	Silty clay with silt	−36.11	10.7	1.63	65	
⑤-4	Silty clay	−38.41	2.3	2.13	65	
⑦	Clay silt	−42.31	3.9	4.28	65	
⑧-1	Silty clay	−47.21	4.9	2.01	60	
⑧-2	Silty soil interbedded with silty clay	−55.17	7.96	7.04	80	3500
⑨	Silt	—		15.21	110	8500

be calculated based on the measured vibration frequency of the stress gauge at the cross section using the following equation:

$$F = \left(E_c A_c + E_s A_s\right) \sum_{j=1}^{n} \frac{\varepsilon_j}{n}, \tag{1}$$

where F is the pile axial force at the calculation section, E_c is the elastic modulus of concrete, E_s is the elastic modulus of steel bar, A_c is the clean cross-sectional area of the concrete pile eliminating the sectional area of reinforcement, A_s is the total area of reinforcement in the pile section, and ε_j is the strain, which is calculated by the following equation:

$$\varepsilon_j = \frac{K\left(f_i^2 - f_0^2\right)}{E_s A_g}, \tag{2}$$

where K is the rate coefficient (kN/Hz^2), f_i is the measured frequency reading at ith stage loading, f_0 is the initial

Table 2: Parameters of physical dimensions and drilling rate for the tested piles.

Tested pile	Pile length (m)	Pile diameter (mm)	Maximum of applied pile load (kN)	Pile head settlement (mm)	Rebounded pile head displacement (mm)	Residual settlement (mm)	Rebounded rate (%)
S-1	55	600 (650–500)	10000	73.49	46.53	26.96	63.3
S-2	55	600 (650–500)	8000	81.88	55.72	26.16	68.1
S-3	55	600 (650–500)	9600	24.01	21.51	2.50	89.6

Drilling rate (m/min)		Thickness of soil layers in process of drilling construction (m)				
		0–20	20–42	42–47	47–52	52–55
Tested piles	S-1	0.92	0.78	0.10	1.41	0.60
	S-2	0.99	0.61	0.29	1.60	1.45
	S-3	0.61	1.22	0.13	1.50	0.61

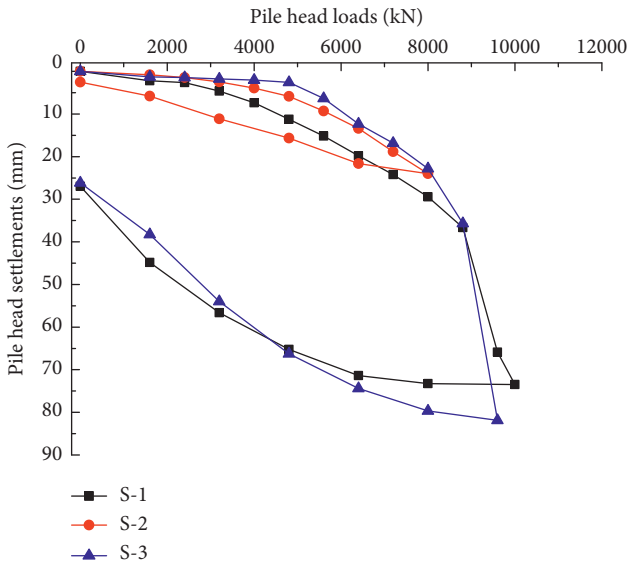

Figure 4: Load-displacement curves of tested piles.

frequency of the embedded gauges, and A_g is the area of single reinforcement. The distributions of the axial pile forces at the section embedding gauges can be obtained by the above equations (1) and (2), shown in Figure 5.

From Figure 5, it can be seen that the axial forces of the three tested piles gradually become smaller along the pile depths with different pile head load levels. At the same depth, the axial pile forces begin to rise with the increasing applied pile head loads.

Side friction along each pile under compression load can be calculated by dividing the difference of two consecutive axial forces by the pile shaft area between the two strain gauges. Therefore, the side friction is an average value corresponding to the distance between the locations of two strain gauges. As a new type of composite pile foundation, in the bearing analysis of static drill rooted nodular piles, PHC piles and cemented soil around the pile are considered as one object when calculating the side friction, due to the high strength cohesion between the pile shaft and surrounding cement. The average pile shaft friction of any two adjacent sections can be obtained by the following equation:

$$f_s = \frac{F_i - F_{i-1}}{\pi d_i \Delta h_i}, \tag{3}$$

where F_i is the axial force at the measured section of i, F_{i-1} is the axial force at the measured section of $i-1$, d_i is the diameter of pile, and Δh_i is the distance between the two tested sections, respectively. The distribution of the average pile side frictions along the test pile is shown in Figure 6.

It can be seen that the mobilizations of the pile side frictions are related to the applied head loads, and the pile side frictions gradually developed with increasing applied pile head loads until the frictions between the pile and surrounding soils are fully mobilized. Figure 6 also shows that it will have a small reduction with the applied load increasing in some soil layers after the pile side frictions are fully developed. It also can be seen in Figure 6 that the pile side frictions are gradually developed fully from the top to the end.

3.3. Analysis of Mobilized Pile End Loads. The mobilized pile base load also can be estimated by equations (1) and (2). The increases of mobilized pile end loads with increasing pile head loads are shown in Figure 7(a), and share ratios of the applied loads at pile heads are shown in Figure 7(b). From Figure 7, it can be seen that the mobilized pile end loads increase approximately linearly with increasing pile head loads except for the destruction phases of the static load tests for pile S-1 and pile S-3.

From Figures 4 and 7 and many tested pile statistics, it can be derived that the relationship between the pile end loads and settlements also can be expressed by the trilinear inear model based on the existing research results (Xie et.al, 2013; Jiang et.al, 2010) [15, 16].

$$P_b = \begin{cases} k_{b1} S_b, & S_b \le S_{ub1}, \\ k_{b1} S_{ub1} + k_{b2} (S_b - S_{ub1}), & S_{ub1} < S_b \le S_{ub2}, \\ k_{b1} S_{ub1} + k_{b2} (S_{ub2} - S_{ub1}), & S_b > S_{ub2}, \end{cases} \tag{4}$$

where P_b is the pile end resistance and S_b is the pile end settlements, and the relationship between the pile end settlements of loads is shown in Figure 8.

When the displacement of the pile end soil is within S_{ub1}, the stiffness of the pile end soil is k_{b1}, and with the increase of

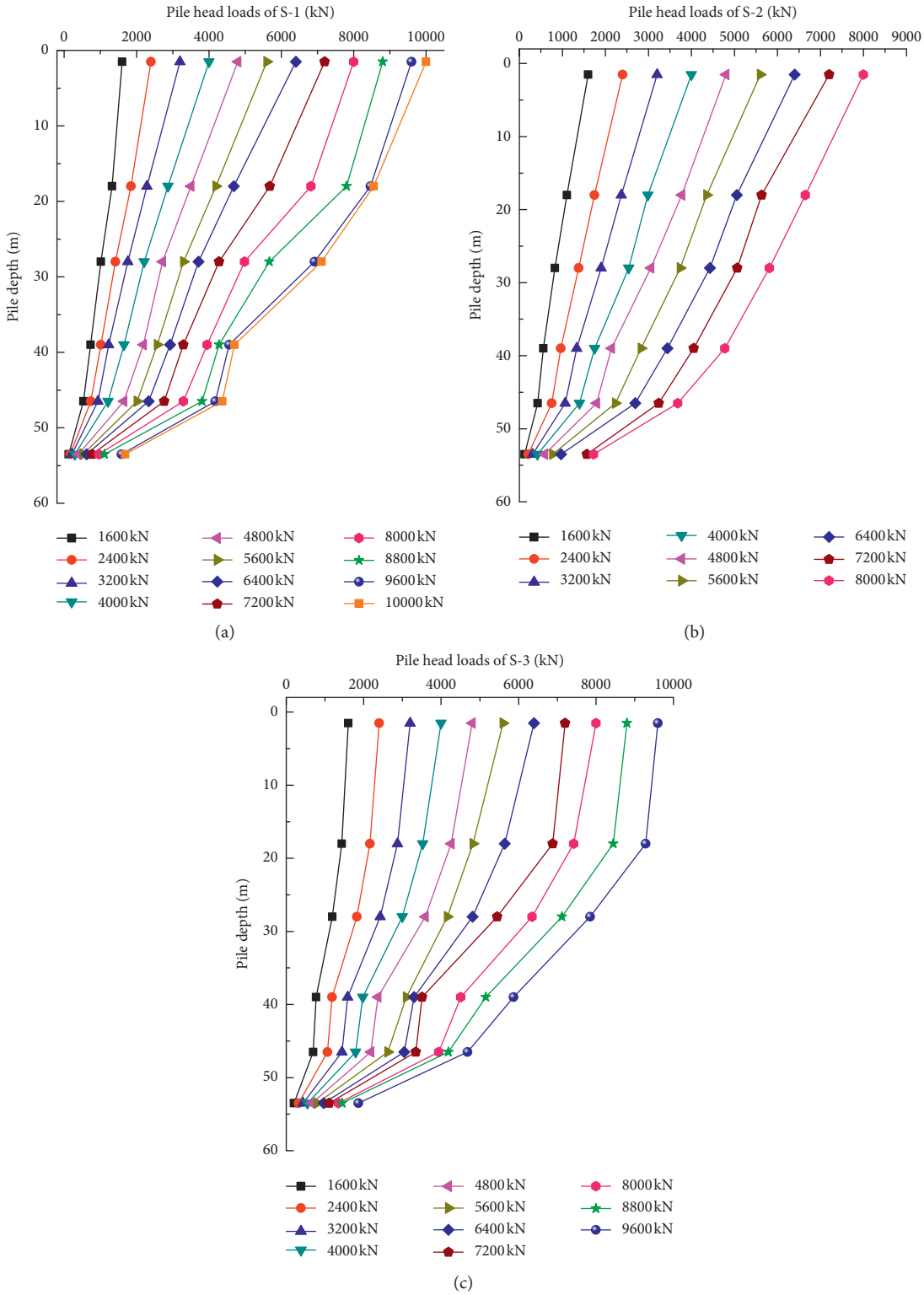

Figure 5: Distributions of axial pile forces.

pile end displacements, the mobilized pile end loads increase linearly. While the value of pile end soil displacements is between S_{ub1} and S_{ub2}, the stiffness of the pile end soil is k_{b2}, and the increase of the pile end loads becomes slower. When the displacement of the pile end soil exceeds the value S_{ub2}, the pile end loads do not change anymore with the displacement of the pile end.

The values of k_{b1} is given by Randolph and Wroth [17]:

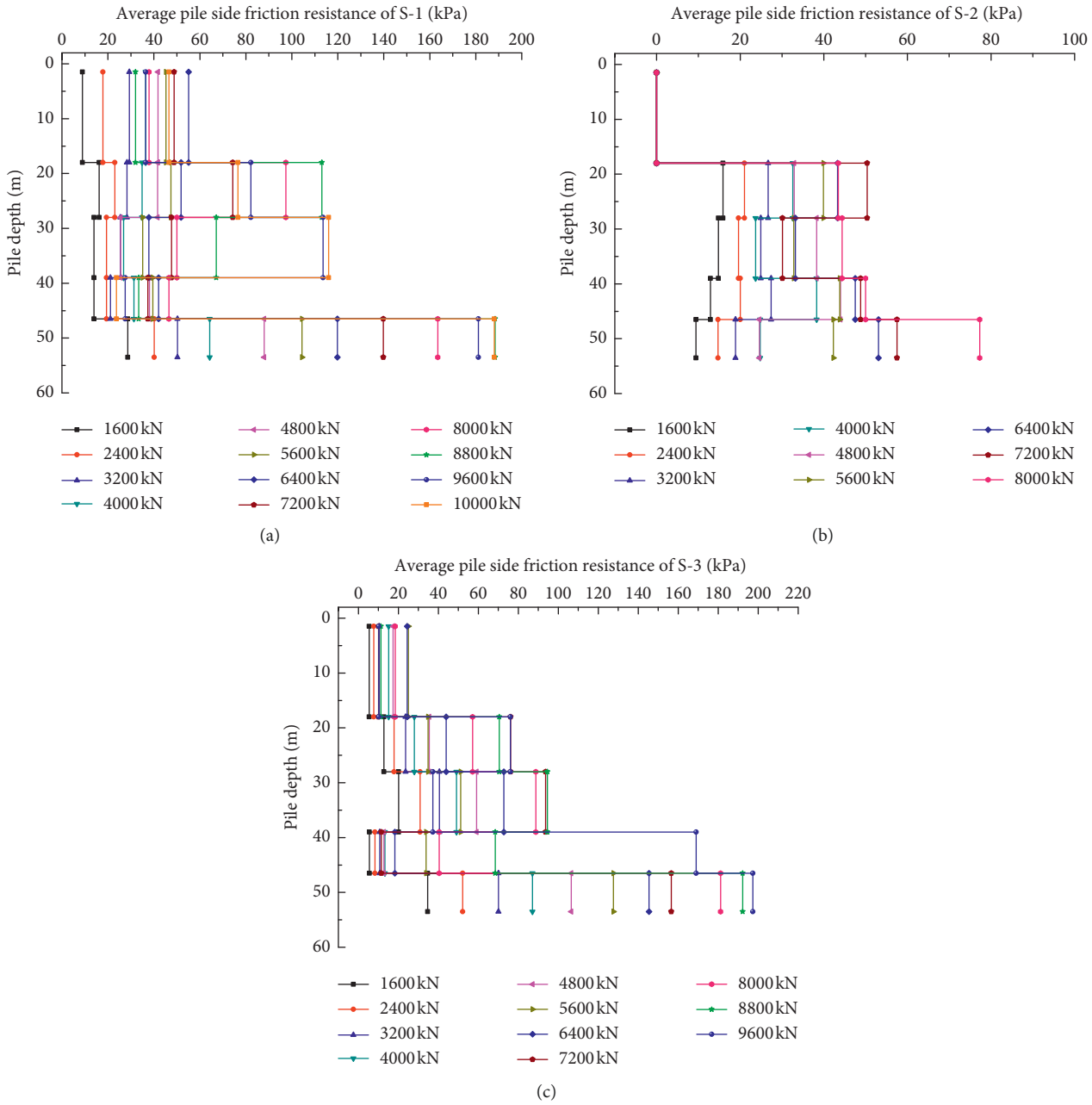

Figure 6: Distributions of average pile shaft frictions.

$$k_{b1} = \frac{4G_{bs}}{\pi r_0 (1 - \nu_{bs})}, \tag{5}$$

where G_{bs} is the shear stiffness and ν_{bs} is Poisson's ratio for the pile base soil.

The value of k_{b2} can be predicted by the measured load-settlement curve. The skin friction is almost fully developed when the settlement at the pile head increases significantly with increasing pile head load. The increased load at the pile head is supported by the pile end resistance. That is, $\Delta p = k_{b2}\Delta s_b$, and the values of k_{b2} are given by

$$k_{b2} = \frac{k_t}{1 - k_t\left(L/E_p A_p\right)}, \tag{6}$$

where k_t is the ratio of the increased load to the increased settlement at the pile head, $k_t = \Delta p/\Delta s_b$ [10].

4. Simplified Calculation Method

Even though many methods about the settlement of pile foundation and load transfer mechanism analysis of single pile exist, these methods for this new-type composite pile are not very applicable due to the existence of cement soils and the interaction of pile, cement soils, and surrounding soils.

The laboratory experimental research studies and engineering measured data show that the mechanical behavior of the pile-soil contact surface is nonlinear [10, 18], and the

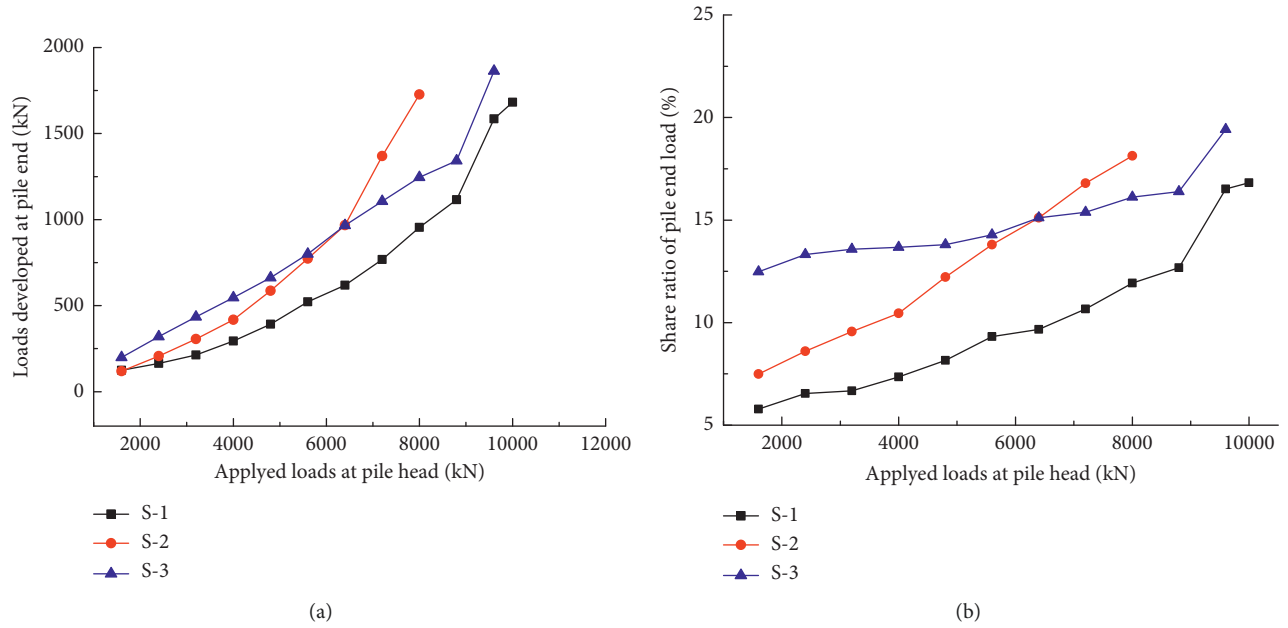

Figure 7: Mobilized pile end loads and share ratios.

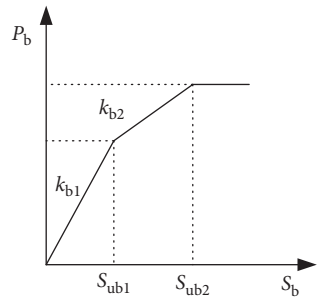

Figure 8: Trilinear model of the relationship between the pile base load and pile base settlement.

nonlinear behavior between the cement soils and surrounding soils in this paper is described by a simple hyperbolic nonlinear model, as shown in Figure 9(a).

From the hyperbolic relationship shown in Figure 9(a), it can be seen that the pile side friction is increasing nonlinearly with gradually increasing applied pile head loads. When the pile-cement soil relative displacement reaches the value, S_u, the shear stress of the pile shaft nearly achieves the limit value, τ_u, and with further increase of the pile head load, the shear stress at the interface of the pile side and surrounding cement soils remains unchanged. This relationship can be expressed as a hyperbolic equation having the following form [10]:

$$\tau(z) = \begin{cases} \dfrac{\Delta s_z}{a + b \times \Delta s_z}, & \Delta s_z \le S_u, \\ \tau_u, & \Delta s_z \ge S_u, \end{cases} \tag{7}$$

where $\tau(z)$ is the shaft shear stress at a given depth z, Δs_z is the pile-soil relative displacement developed in the pile-soil interface at a given depth z, and a and b are empirical coefficients whose values are determined experimentally or by back analysis of field test results. The reciprocal of coefficient a can be considered as the initial stiffness of the shaft shear stress-relative displacement relationship at the pile-soil interface as shown in Figure 8. The reciprocal of coefficient b is the asymptote of the shaft shear stress-displacement curve at a very large value of relative displacement, S_u. This asymptote shaft shear stress τ_u is slightly greater than the maximum possible value of the pile-soil interface τ_f. The pile displacement along pile depth in the pile-soil interface ignoring the displacement of surrounding soils at ith calculation segment can be obtained by the following equation:

$$S_i = S_t - \sum_{j=1}^{i} \frac{L_j}{2}\left(\varepsilon_j + \varepsilon_{j+1}\right), \tag{8}$$

where L_j is the length of pile shaft located at section j, S_t is the pile head settlement, and ε_j and ε_{j+1} are the strain of the reinforcing steel bar of the jth and $(j+1)$ th segments, respectively [10, 19].

As the asymptote of the shear stress τ_u, the coefficient b is slightly greater than the peak strength at the pile-soil interface τ_f. The shear stress, τ_u, is expressed in terms of τ_f by the parameter of failure ratio, R_f, as shown in the following equation:

$$\tau_f = R_f \tau_u. \tag{9}$$

The values of R_f for the shear stress-relative displacement curve are found to be in the range of 0.8–0.95 [9, 10, 20].

The shear strength at the interface is proportional to the normal stress, and the strength characteristics at the interface can be expressed in terms of the friction angle of the pile shaft-soil interface, θ, as follows:

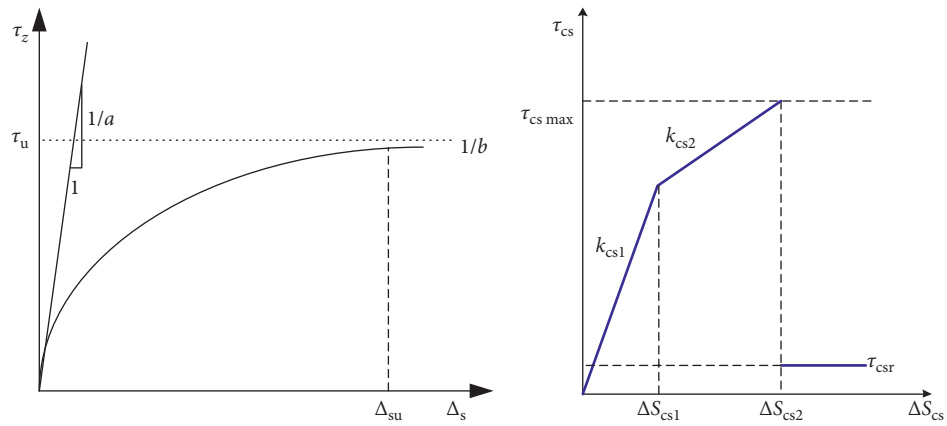

Figure 9: The relationship between shear stress and relative displacement of pile shaft.

$$\tau_f = \sigma_n \tan\theta. \tag{10}$$

Thus, the value of coefficient b can be written as

$$b = \frac{R_f}{\sigma_n \tan\theta}. \tag{11}$$

The coefficient a, as reciprocal of the initial stiffness of the shaft stress-relative displacement relationship at the pile-soil interface, can be obtained as [9, 10, 17]

$$a = \frac{r_0 \ln(r_m/r_0)}{G_s}. \tag{12}$$

As shown in Figure 9(b), the contact behavior between the PHC pile and surrounding cement soils in this paper is described by a simple bilinear and sudden dropping model based on the laboratory test results by Zhou [5, 6]. From the relationship of the shear stress at the PHC pile shaft and the relative displacement, as shown in Figure 9(b), it can be seen that the contact friction increases linearly with increasing relative displacement before the relative displacement reaching the first limit value, Δs_{cs1}. When the value of relative displacement is between Δs_{cs1} and Δs_{cs2}, the stiffness becomes k_{sc2}, and when the relative displacement between the PHC pile shaft and surrounding cement soils exceeds the value Δs_{cs2}, the contact friction becomes τ_{csr} suddenly with increase of the relative displacement:

$$\tau(z)_{cs} = \begin{cases} k_{cs1}\Delta s_{cs}, & \Delta s_{cs} < \Delta s_{cs1}, \\ k_{cs1}\Delta s_{cs1} + k_{cs2}(\Delta s_{cs} - \Delta s_{cs1}), & \Delta s_{cs1} \le \Delta s_{cs} < \Delta s_{cs2}, \\ \tau_{csr}, & \Delta s_{cs} \ge \Delta s_{cs2}. \end{cases} \tag{13}$$

The values of coefficients k_{cs1} and k_{cs2} depend on the properties of the cement soil which is decided by the properties of the soil stratum. The value of coefficients k_{cs1} is between 130 kPa/mm and 150 kPa/mm, and the value of coefficient k_{cs2} is between 30 kPa/mm and 70 kPa/mm, and the residual strength τ_{csr} is about 20 kPa, obtained from the studies of Zhou et al. [5] by back analysis.

The nonlinearity of the surrounding soils is developed essentially at the interface between the cement soils and the surrounding soils at a given depth below the ground surface, confining to a very narrow zone of the soils close to the cement soils, and the interaction between other elements may be represented by a linear model with sufficient accuracy [21–24]. The total displacement of the soils surrounding the pile shaft, s_z, at depth z can be expressed in the following form [8, 9]:

$$s_z = \Delta s_z + w_{sz}, \tag{14}$$

where Δs is the nonlinear displacement mobilized by the shaft stresses τ_z confined to the narrow disturbed soil around the cement soils and w_{sz} is the purely elastic displacement outside the narrow disturbed zone. The relationship between Δs and w_{sz} is shown in Figure 10.

The elastic displacement of soil surrounding the cement soils w_{sz} induced by the shaft shear stresses can be expressed by the elastic solution proposed:

$$w_{sz} = \frac{r_0}{G_s}\tau_z \ln\left(\frac{r_m}{r_0}\right) = c\tau_z, \tag{15}$$

where r_0 is the radius of the cement soils; G_s is the shear modulus of the soil outside the disturbed zone; and c is a parameter, which satisfies $c = r_0/G_s \ln(r_m/r_0)$, where r_m is the radius distance from the pile center to a point at which the shear stress induced by the pile can be considered to be negligible. According to Randolph and Wroth, the values of r_m can be taken as $r_m = 2.5L(1 - 0.5\nu_s)$, where L is the length of the pile and ν_s is Poisson's ratio of the soil [9, 10, 17, 19, 20, 25].

At the lower part of the static drill rooted pile with bamboo joint pile and cement soil with length of L_1, the bamboo joint pile and cement soil are considered as a whole part in the calculation process due to the reinforcement of nodular section to the surrounding cement soils and the high strength cohesion between the pile shaft and surrounding cement. In the upper part of the static drill rooted pile with length of L_2, the relative displacement between PHC pile and

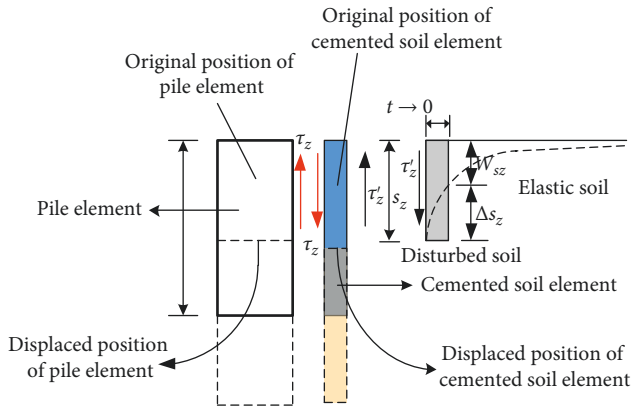

FIGURE 10: Idealized displacement developed around a pile element.

surrounding cement soil is considered, as shown in Figure 11(a).

As shown in Figure 11(b), the pile base is origin of coordinate, and the depth at the calculated section of bamboo joint pile is z, and the length of bamboo joint pile is L_1. For the moment, the load transfer curves are assumed to be linear, and k_s is initial shear stiffness in the units of kN/m^3 associated with unit length. Assuming that, the pile base settlement is Δ_b, with extremely small value about 10^{-2} mm. It is noted that the settlement at the calculating section of the pile consists of the compression of the composite pile shaft and pile base settlement.

The total settlement at depth z is as a sum of the above two parts and can be written as

$$\int_0^z \frac{P_z}{E_{sp}A_{sp}}dz + \Delta_b, \tag{16}$$

where E_{sp} is the average modulus of the PHC pile or bamboo joint pile and cement soils and A_{sp} is the total area of the PHC pile and cement soil, which are calculated as follows:

$$E_{sp} = \frac{E_pA_p + E_{cs}A_{cs}}{A_{sp}}, \tag{17}$$

where E_p is the modulus of the PHC pile or bamboo joint pile and E_{cs} is the modulus of cement soils and A_p is the area of the PHC pile or bamboo joint pile and A_{cs} is the area of cement soil, respectively.

Also, the total pile shaft shear stress of this calculated segment can be expressed in the following form:

$$f = k_s\int_0^z\left(\int_0^z \frac{p_z}{E_{sp}A_{sp}}dz - c\tau_z + \Delta_b\right)dz. \tag{18}$$

The axial force at depth z, p_z, can be written as

$$p_z = k_b\Delta_b + k_s\int_0^z\left(\int_0^z \frac{p_z}{E_{sp}A_{sp}}dz + \Delta_b - c'p'_z\right)dz, \tag{19}$$

where $c = 2\pi r_0c'$, and the following expression can be obtained:

$$(1 + ck_s)p''_z = \frac{k_s}{E_{sp}A_{sp}}p_z. \tag{20}$$

The solution to the above second-order differential equation can be obtained by substituting the boundary conditions $p_0 = k_b\Delta_b$, $p'_0 = k_s\Delta_b/(1 + k_sc)$ into the general solutions of differential equations of equation (20):

$$p_z = \frac{\alpha}{2}\Delta_be^{hz} + \frac{\beta}{2}\Delta_be^{-hz}, \tag{21}$$

where $h^2 = k_s/E_{sp}A_{sp}(1 + c'k_s)$, $\alpha = k_b + hE_{sp}A_{sp}$, $\beta = k_b - hE_{sp}A_{sp}$.

The pile shaft settlement at depth z can be obtained from equation (16):

$$\Delta_z = \frac{p_z}{E_{sp}A_{sp}h}\frac{\alpha e^{hz} - \beta e^{-hz}}{\alpha e^{hz} + \beta e^{-hz}}. \tag{22}$$

The settlement of the surrounding soils is written in the following form:

$$w_{sz} = c'p_zh\frac{\alpha e^{hz} - \beta e^{-hz}}{\alpha e^{hz} + \beta e^{-hz}}. \tag{23}$$

The relative displacement, Δs, along the pile shaft at the depth z can be simulated using the following equation:

$$\Delta s_z = \frac{p_zh}{k_s}\frac{\alpha e^{hz} - \beta e^{-hz}}{\alpha e^{hz} + \beta e^{-hz}}. \tag{24}$$

From the bamboo joint pile head that is also the PHC pile tip, the relative displacement between the PHC pile and surrounding cement soil is considered. From the total equilibrium for the side contact frictions of the PHC pile, cement soils, and surrounding soils, the side friction between cement soil and PHC pile shaft for the upper part of the whole piles can be obtained by the following equation:

$$\tau_{pcz} = \frac{p_z - p_{L_1}}{\pi d_p(L_z - L_1)}, \tag{25}$$

where τ_{pcz} is the side friction between cement soil and PHC pile shaft, L_z is the calculated position, p_z is the obtained pile force at calculated position, p_{L_1} is pile force at bamboo joint pile head, and d_p is diameter of PHC pile. The relative displacement between cement soil and PHC pile can be obtained by back analysis of equation (13), considering the equilibrium of total frictional resistance at pile side. In nondestructive loading conditions, the relative displacement between cement soil and surrounding soils is relatively larger than that between cement soil and PHC pile shaft.

As applied loads at pile head increase, the relative displacement between cement soils and surrounding soils increases and the load transfer curves for the cement soils and surrounding soils become nonlinear. The relative displacement between the PHC pile or bamboo joint pile and surrounding cement soils is always in the first elastic stage, as shown in Figure 9(b). In order to get effective and accurately solution, the pile can be divided into adequate segments of n, as shown in Figure 11(b); the corresponding axial force of the calculating section at the depth z can be obtained:

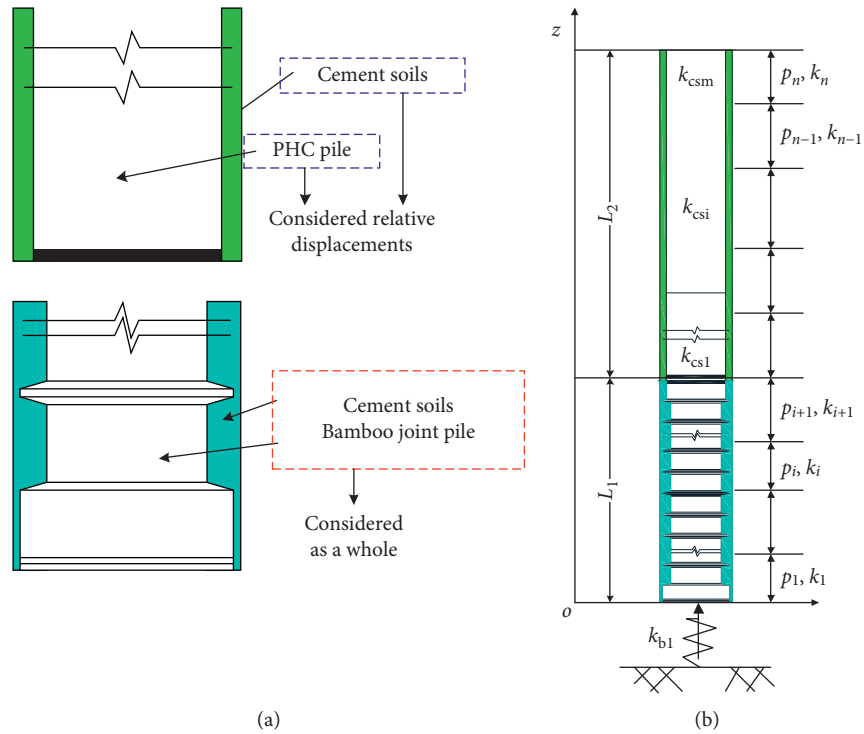

Figure 11: Calculation model for pile settlement analysis.

Table 3: Soil profile and parameters for the tested piles.

Name of soil layer	Thickness of soil layer (m)	a (mm/kPa)	b (kPa^{-1})	τ_u (kPa)	k_{sc1} (mm/kPa)
Miscellaneous fill	1.09				
Silty clay	1.4	$6.69E-2$	$4.53E-2$	17.96	
Sandy silty soil	3.3	$3.88E-2$	$2.78E-2$	33.41	
Muddy silty clay	3.9	$3.31E-2$	$2.80E-2$	46.17	
Muddy clay	9.53	$2.99E-2$	$3.15E-2$	60.01	
Silty clay	8.37	$2.72E-2$	$2.49E-2$	73.75	150
Silty clay with silt	10.7	$4.53E-2$	$2.01E-2$	88.34	
Silty clay	2.3	$1.38E-2$	$1.023E-2$	105.51	
Clay silt	3.9	$4.19E-2$	$9.72E-3$	102.93	
Silty clay	4.9	$2.12E-2$	$7.69E-3$	119.24	
Silty soil interbedded with silty clay	7.96	$2.10E-2$	$7.54E-3$	118.95	
$k_{b1} = 113.30$ (kN/mm), $s_{ub1} = 4$ (mm)		$k_{b2} = 66.24$ (kN/mm), $s_{ub2} = 20.9$ (mm)			$\Delta s_{cs1} = 1$ mm

$$p_{zi} = \frac{\alpha_i}{2}\Delta_{b_i} e^{h_i z_i} + \frac{\beta_i}{2}\Delta_b e^{-h_i z_i}. \quad (26)$$

And the corresponding axial settlement at the calculating section at the depth z can be obtained:

$$\Delta_{zi} = \frac{p_{zi}}{E_{sp_i} A_{sp_i} h_i} \frac{\alpha_i e^{h_i z_i} - \beta_i e^{-h_i z_i}}{\alpha_i e^{h_i z_i} + \beta_i e^{-h_i z_i}}. \quad (27)$$

The corresponding virtual stiffness at the calculated segment head can be obtained by the following expression:

$$k_i = E_{sp_i} A_{sp_i} h_i \frac{\alpha_i e^{h_i z_i} + \beta_i e^{-h_i z_i}}{\alpha_i e^{h_i z_i} - \beta_i e^{-h_i z_i}}, \quad (28)$$

where $h_i^2 = k_{s_i}/E_{sp_i} A_{sp_i} (1 + c' k_{s_i})$, $\alpha_i = k_{b_i} + h_i E_{sp_i} A_{sp_i}$, $\beta_i = k_{b_i} - h_i E_{sp_i} A_{sp_i}$.

In multilayered soils, the calculation model, as shown in Figure11(b), can be used to predict the settlements and pile shaft load distribution. The changes of stiffness in the calculation can be obtained by equations (4), (7), and (13). Calculate the axial force of the pile at top of the computing pile segment, p_n, using equation (21), and the settlement at the top of corresponding layer soil Δ_n, using equation (22). The relative displacement between cement soils and surrounding soils can be estimated by equation (24), and the relative displacement between PHC pile and cement soils can be calculated using equation (13). Use the modified parameters obtained in the above steps to calculate the axial forces and settlements of each pile segments by repeating the above steps for the next calculation step.

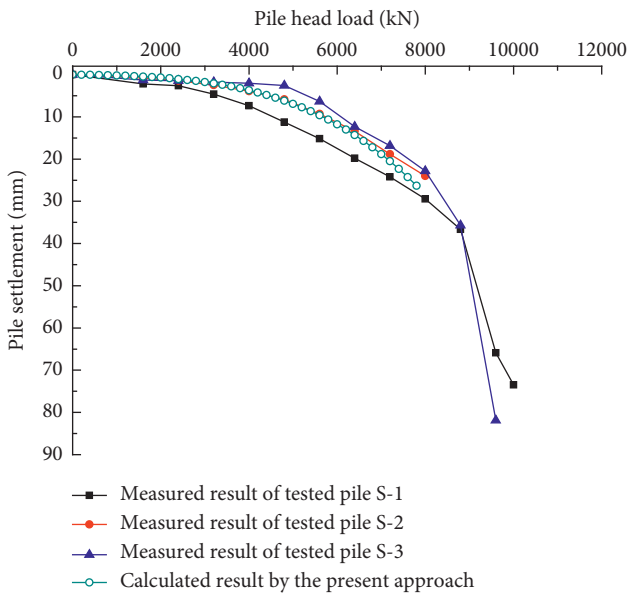

Figure 12: Comparison of load-settlement between the measured and computed results for a single pile.

5. Comparison

The proposed method for the prediction of a single static drill rooted pile is used to analyze field loading tests reported in this paper, and the comparisons between the calculated results with those measured in full load tests are given.

The site test pile of S-2 was a static drill rooted pile, with length of 55m. The diameter of PHC pile is 600m and the type of bamboo joint pile is 650(500)mm type. The value of R_f is assumed to be 0.90 for the whole deposit. The other parameters, obtained approximately by back analysis of the measured results using the equation (7), are listed in Table 3.

Comparisons of the curves computed by the proposed approach and measured load-settlement results are shown in Figure 12. Figure 12 shows that the load-settlement relationship at the pile head, calculated by the present method, is generally consistent with the measured result.

6. Conclusion

Three in situ tests on static drill rooted piles were carried out to explore the bearing characteristics of the new-type SDRN pile foundation. The axial forces of the three test piles are observed decreasing smoothly along the pile depths regardless of load levels, while the axial stress at the same pile depth grows with the increasing vertical loads. The mobilizations of the pile side frictions are related to the applied head loads, and the pile side frictions gradually developed with increasing applied pile head loads until the frictions are fully mobilized. The mobilized pile end loads increase approximately linearly with increasing pile head loads before reaching the ultimate loads. The pile end load-settlement curves can be expressed by the trilinear model, the relationship between the cement soils and surrounding soils is simulated by hyperbolic function, and the relationship between cement soils and PHC pile is described by a simple bilinear and sudden dropping model. Based on the analysis of on-site tests and above assumption, a simplified approach was proposed to estimate pile axial force and displacement along pile depth. The comparisons between calculated results with measured results show that the proposed approach can be used to predict the settlement and capacity of this new-type pile foundation.

Data Availability

All the data used to support the findings of this study are included within the article.

Conflicts of Interest

The authors declare that there are no conflicts of interest regarding the publication of this paper.

Acknowledgments

This research was supported by the National Natural Science Foundation of China (research grant nos. 51708496 and 51708497) and the Zhejiang Provincial Natural Science Foundation (research grant nos. LY16E080010 and LQ19E080009). These financial supports are gratefully acknowledged.

References

[1] X. N. Gong and X. H. Li, "Several mechanical problems in compacting effects of static piling in soft clay ground," *Engineering Mechanics*, vol. 17, no. 4, pp. 7–12, 2001, in Chinese.

[2] H. Y. Zhou and J.-Y. Shi, "Test research on soil compacting effect of full scale jacked-in pile in saturated soft clay," *Rock and Soil Mechanics*, vol. 30, no. 11, pp. 3291–3296, 2009, in Chinese.

[3] O. Borda, M. Uno, and I. Towhata, "Shaft capacity of nodular piles in loose sand," *Proceedings of the 49th National Conference, Japanese Geotechnical Society, Japan*, vol. 2, pp. 1175-1176, 2007, in Japanese.

[4] R. H. Zhang, L. L. Wu, and Q. H. Kong, "Research and practice of JZGZ pile foundation," *Chinese Journal of Geotechnical Engineering*, vol. 35, pp. 1200–1203, 2013, in Chinese.

[5] J.-J. Zhou, X.-N. Gong, K. H. Wang, and R. H. Zhang, "A field study on the behavior of static drill rooted nodular piles with caps under compression," *Journal of Zhejiang University Science A*, vol. 16, no. 12, pp. 951–963, 2015.

[6] J.-J. Zhou, *Test and Modeling on Behavior of the Pre-Bored Grouting Planted Nodular Pile*, Zhejiang University, Hangzhou, China, 2016.

[7] F. Castelli and M. Maugeri, "Simplified nonlinear analysis for settlement prediction of pile groups," *Journal of Geotechnical and Geoenvironmental Engineering*, vol. 128, no. 1, pp. 76–84, 2002.

[8] K. M. Lee and Z. R. Xiao, "A simplified nonlinear approach for pile group settlement analysis in multilayered soils," *Canadian Geotechnical Journal*, vol. 38, no. 5, pp. 1063–1080, 2001.

[9] Z. Wang, X. Xie, and J. Wang, "A new nonlinear method for vertical settlement prediction of a single pile and pile groups in layered soils," *Computers and Geotechnics*, vol. 45, pp. 118–126, 2012.

[10] Q.-Q. Zhang, Z.-M. Zhang, and J.-Y. He, "A simplified approach for settlement analysis of single pile and pile groups considering interaction between identical piles in multilayered soils," *Computers and Geotechnics*, vol. 37, no. 7-8, pp. 969–976, 2010.

[11] H. B. Seed and L. C. Reese, "The action of soft clay along friction piles," *Transactions of the American Society of Civil Engineers*, vol. 122, pp. 731–754, 1957.

[12] S. Armaleh and C. S. Desai, "Load-deformation response of axially loaded piles," *Journal of Geotechnical Engineering*, vol. 113, no. 12, pp. 1483–1500, 1987.

[13] L. M. Kraft, R. P. Ray, and T. Kakaaki, "Theoretical t–z curves," *Journal of the Geotechnical Engineering Division*, vol. 107, no. 11, pp. 1543–1561, 1981.

[14] JGJ 106-2014, *Technical Code for Testing of Foundation Piles*, Ministry of Housing and Urban-rural Development, Beijing, China, 2014, in Chinese.

[15] J. Q. Jiang, Y. S. Zang, and G. Y. Gao, "Study on bearing behaviors of pile tip resistance of super-length piles," *Engineering Mechanics*, vol. 27, no. 2, pp. 149–160, 2010.

[16] X. Y. Xie, Z. J. Wang, and J. C. Wang, "Calculation method for settlement of super-long pile considering nonlinearity of pile and soils," *Journal of Central South University (Science and Technology)*, vol. 44, no. 11, pp. 4464–4471, 2013, in Chinese.

[17] M. F. Randolph and C. P. Wroth, "An analysis of the vertical deformation of pile groups," *Géotechnique*, vol. 29, no. 4, pp. 423–439, 1979.

[18] A. Mandolini and C. Viggiani, "Settlement of piled foundations," *Géotechnique*, vol. 47, no. 4, pp. 791–816, 1997.

[19] Q.-Q Zhang, L. Shan-wei, F. Ruo-Feng, and X. M. Li, "Analytical method for prediction of progressive deformation mechanism of existing piles due to excavation beneath a pile-supported building," *International Journal of Civil Engineering*, vol. 17, no. 6, pp. 751–763, 2019.

[20] G. W. Clough and J. M. Duncan, "Finite element analysis of retaining wall behavior," *Journal of the Soil Mechanics and Foundations Division*, vol. 97, no. 12, pp. 1657–1673, 1971.

[21] V. Caputo and C. Viggiani, "Pile foundation analysis: a simple approach to nonlinearity effects," *Rivista Italiana di Geotecnica*, vol. 18, no. 1, pp. 32–51, 1984.

[22] Y. K. Chow, "Analysis of vertically loaded pile groups," *International Journal for Numerical and Analytical Methods in Geomechanics*, vol. 10, no. 1, pp. 59–72, 1986.

[23] Y. F. Leung, K. Soga, B. M. Lehane, and A. Klar, "Role of linear elasticity in pile group analysis and load test interpretation," *Journal of Geotechnical and Geoenvironmental Engineering*, vol. 136, no. 12, pp. 1686–1694, 2010.

[24] A. M. Trochanis, J. Bielak, and P. Christiano, "Three-dimensional nonlinear study of piles," *Journal of Geotechnical Engineering*, vol. 117, no. 3, pp. 429–447, 1991.

[25] Q.-Q Zhang, F. Ruo-Feng, L. Shan-wei, and X. M. Li, "Estimation of uplift capacity of a single pile embedded in sand considering arching effect," *International Journal of Geomechanics*, vol. 18, no. 9, article 06018021, 2018.